TIME-SERIES ANALYSIS OF SATELLITE IMAGES FOR FOREST COVER CHANGE MONITORING IN TANZANIA

Øivind Due Trier[1] and Arnt-Børre Salberg[1]

1. Norwegian Computing Center, Gaustadalléen 23, P.O. Box 114 Blindern, NO-0314 Oslo, Norway; e-mail trier@nr.no, salberg@nr.no

ABSTRACT

Nation-wide forest cover change monitoring in countries the size of Tanzania needs to be based on automatic processing chains. Whenever new satellite images are available, they should be processed to provide updated estimates of deforestation, reforestation, forest degradation and regeneration. This paper describes some of the methods that will be used in a Norwegian-funded project to enhance the measuring, reporting and verification of forests in Tanzania through the use of advanced remote sensing techniques. Landsat-5 TM and -7 ETM+ images provide the main source of satellite data, supplemented by SAR images to reduce the impact of cloud cover. The Norwegian Computing Center (NR) is responsible for developing methods for pre-processing of optical images and automatic forest change detection in time series of optical images. NR will also contribute in extending the change detection method to combine optical and SAR images in the time series.

The pre-processing of optical images includes atmospheric correction, cloud and cloud shadow detection and masking, and co-registration and terrain height correction. Forest change detection is based on a hidden Markov model. In this context, "hidden" refers to the fact that the true land cover state for each location on the ground is unknown, but observations are available as a time series of satellite image pixels. Given the observations, the most probable sequence of ground cover states is determined. From this, forest state changes, say, from "forest" to "non-forest", can be found to have occurred between two observations. Due to varying cloud cover across a scene, and missing pixels (SLC-off) in Landsat 7 due to sensor failure, the different pixels may have different time series of observations. The hidden Markov model automatically compensates for this. However, the accuracy will increase with more observations, so it is important to have access to a dense time series of past observations, and guaranteed access to future acquisitions at regular and relatively short time intervals. The upcoming Landsat-8 and Sentinel-2 optical satellites will be important in this respect.

INTRODUCTION

The Government of Norway has entered into a bilateral agreement with the Government of Tanzania on Climate and Forest. The overall goal of this agreement is to achieve reductions in greenhouse gas emissions from deforestation and forest degradation in Tanzania. The introduction of a measuring, reporting and verification (MRV) system that meets the United Nations Framework Convention on Climate Change (UNFCCC) reporting requirements is a vital part of this agreement.

Nation-wide forest cover change monitoring in countries the size of Tanzania needs to be based on automatic processing chains. Whenever new satellite images are available, they should be processed to provide updated estimates of deforestation, reforestation, forest degradation and regeneration. This paper describes some of the methods that will be used in a Norwegian-funded project to enhance the measuring, reporting and verification of forests in Tanzania through the use of advanced remote sensing techniques. Landsat-5 TM and -7 ETM+ images provide the main source of satellite data, supplemented by SAR images to reduce the impact of cloud cover. The Norwegian Computing Center (NR) is responsible for developing methods for pre-processing of optical images and automatic forest change detection in time series of optical images. NR will also

contribute in extending the change detection method to combine optical and SAR images in the time series.

One task in this project is to develop methods for improved atmospheric correction of high resolution optical images, for use in an operational setting, both for historical and current images. Ideally, one is interested in vegetation and ground surface reflectance, with all atmospheric effects eliminated, in order to be able to accurately monitor changes of vegetation on the ground. Further, it is desirable to be able to measure surface reflectance using different high resolution optical sensors. This requires sensor cross-calibration, or at least, that the differences between sensors are studied.

Atmospheric correction to surface reflectance is not a trivial task, and many methods have been suggested (see, e.g., (1)). One popular atmospheric correction method is based on dark objects that are identified in the image, and used to estimate the aerosol optical thickness. The dark dense vegetation method by Kaufman et al. (2) is such a method, and was applied by the Landsat Ecosystem Disturbance Adaptive System (LEDAPS) (3). An alternative is to use images from other satellites to assist in the calibration of the Landsat images (see, e.g., (4)). The MODIS sensor on board the Terra satellite acquires images 45 minutes after the Landsat-5 TM sensor, and for the Landsat 7 ETM+-sensor, the time difference is 15 minutes. Some of the 36 MODIS bands are designed for atmospheric correction of water vapour, aerosols and haze, and could be utilized in atmospheric correction of Landsat images as well, provided the conditions have not changed significantly (in a statistical sense) between the MODIS and Landsat acquisitions. MODIS has operated since 2000, so for pre-2000 Landsat scenes, MODIS cannot be used. One candidate instrument is ATSR-2, on board ERS-2, which has operated since 1995. Another candidate, AVHRR has operated since 1978. Both these instruments have only a few channels, and low resolution, so one may have to resort to a semi-automatic atmospheric correction procedure for pre-2000 Landsat scenes. The upcoming medium resolution Sentinel-3 has dedicated channels for atmospheric correction, so the MODIS-Landsat combination approach will give relevant experience on how Sentinel-3 can be used to improve atmospheric correction of high resolution images from Sentinel-2 and Landsat-8.

For optical images, clouds and cloud shadows often obscure parts of the image. These need to be detected and labelled as missing data. This enables subsequent methods to make their own decisions about how missing data should be handled. Since a thermal band is included in the Landsat sensor, many good cloud detection algorithms have been proposed for Landsat images (5). However, robust detection of cloud shadows is not trivial, but good estimates may be obtained by using information about the cloud position and location of the Sun (6).

There are a number of alternatives to handle missing data. One approach is to fill in missing image portions from previous acquisitions of the same area on the ground, either from the same satellite sensor or from another sensor. Alternatively, one may design the subsequent classification/detection methods to handle missing data by using time series analysis. However, the particular strategy can be different in different systems, so the pre-processing methods should not make these decisions. The pre-processing step should only flag these areas as missing, preferably labelling the cause of the data being missing.

An important design principle in this project is to use automatic processing of time series of satellite images. The motivation is that automatic (forest) land cover classification cannot be performed reliably on a single (cloud free) remotely sensed image for a number of reasons. Thus, an attempt at doing automatic change detection from two land cover maps of the same scene at two different dates is even less reliable, as the errors from the two classifications add up. Rather, a time series of many acquisitions of each scene is needed to account for the inherent variability due to seasonal (phenological) variations of ground cover reflectance, varying atmospheric disturbances, humidity on the ground, etc. In the time series analysis approach, the natural variations can be modelled, and distinct deviations from the expected natural variability will be flagged as changes. The time series analysis will then also be able to produce:

1.   minimum cloud cover mosaics, adjusted to the correct phenological state for a given date;

2.   land cover classification,

3.   forest/non-forest map, and/or

4.   per cent tree cover.

These single-date products will emerge as an output from the time series analysis, not the other way around. Single date products may be produced more accurately if one considers a time series of images and model the natural variation of the land cover and measurement noise.

As a result, the pre-processing steps in this project are limited to steps that do not preclude subsequent time series analysis of the images. As a consequence, mosaicking or gap filling will not be part of the pre-processing.

An important goal in the project is to provide methods to map forest areas and forest area changes on a yearly basis for the whole of Tanzania. For this purpose, the only available data source with full national coverage is satellite data. In addition, forest land cover and changes need to be established for historic data on five-year intervals from 1980 to date.

The motivation for using time series of remote sensing images is to detect changes of vegetation with high degree of certainty (7). By using time series we may be able to discriminate between natural variability and changes caused by human activity, and eliminate seasonal variability. Trends can then be estimated with a higher degree of certainty. Time series have been used in the literature to increase the performance of land cover classification by including acquisitions from several phenological states. Aurdal et al. (8) and Leite et al. (9) used hidden Markov models to account for the phenological variation during a year, and thus increased the classification performance. Salberg (10) used a pixel level fusion approach on a stack of Landsat acquisitions to strengthen the classification results, assuming no changes of land cover between image acquisitions.

An important first task is to study the natural variability of ground cover reflectance for different land cover classes. What is the natural variability, and how do the ground cover reflectance and the phenological states vary within the same geographical area and between different geographical areas? Such a study requires access to a large image database.

The observed natural variability must be used to tune the time series analysis methods, which are used for change detection and production of single-date products. One approach is to identify areas on the ground that maintain the same land cover class through a number of image acquisitions, and use these to calibrate the time series analysis methods. Then the time series methods can adapt to the observed natural variability.

As mentioned earlier, single date products can be produced as output from the time series analysis. This can be done by e.g. finding the optimal land cover sequence for each pixel using the Viterbi algorithm (11), or by finding the optimal land cover for a given date using the forward-backward or BJCR-algorithm (12,13). Single date products include:

1. land cover map,

2. forest/non-forest map,

3. per cent tree cover, and

4. minimum cloud cover mosaic.

Typically, one wishes to produce annual land cover maps, etc. For areas with phenological variations during one year (due to deciduous trees or otherwise), one can use a land cover product to predict the ground cover reflectance at any date, and produce a synthetic minimum cloud cover image mosaic for a specific date.

An expected outcome of this project is methods and systems for producing historic and current changes of forest areas in Tanzania, and for producing land cover maps, forest/non forest maps, per cent tree cover maps, and minimum cloud cover image mosaics. The goal is that these methods and systems can enable Tanzania to document historical and annual changes in forest areas, in accordance with the reporting guidelines of the UNFCCC.

DATA AND METHODS

In order to assess the suitability of the hidden Markov model, a small experiment is conducted on a time series of Landsat optical satellite images.

Satellite data

A stack of 14 Landsat TM L1T images (path 166, row 063) are being used, covering a 196 km x 182 km area, half of which is ocean. The land area is a part of Tanzania, including the Nilo Forest Reserve in the south-western part of the image. The forest reserve contains intact tropical forest, but just outside of the reserve boundary there are areas with changing land cover. Five images are from 1985-1987, three images are from 1995, and six images are from 2008-2010 (Figure 1). The images are available from the U. S. Geological Survey (USGS) at http://earthexplorer.usgs.gov. All images are converted to top-of-the-atmosphere reflectance and level 1T terrain corrected. Upon visual inspection, all the images used in this study appear to be correctly geo-referenced and co-registered to sub pixel accuracy.
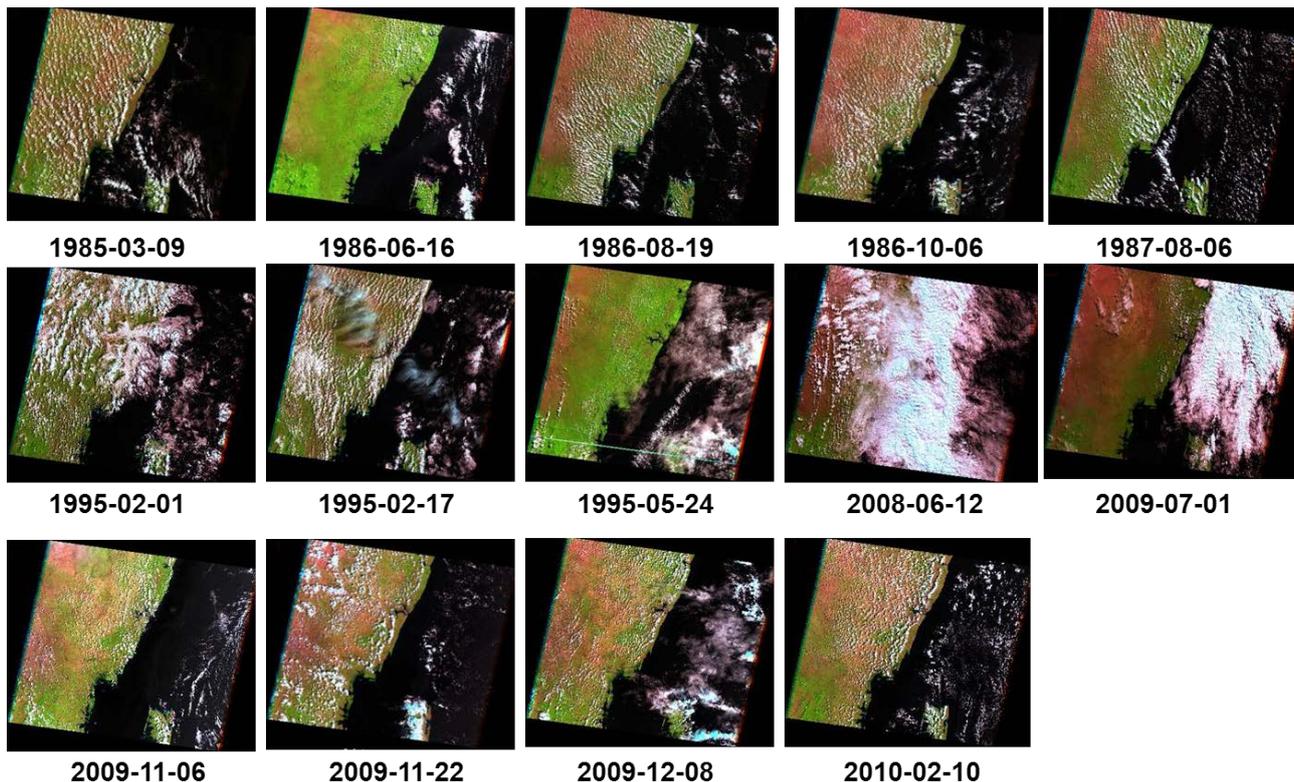

Figure 1. The Landsat images used in this study.

We also have access to a Worldview-2 image from 4 March 2010 (Figure 2), provided free of charge by Digital Globe, Inc., as part of the Group on Earth Observations (GEO) Forest carbon Tracking (FCT) data acquisition for national demonstrators. The Worldview-2 image covers a small part of the Landsat image stack, including parts of the Nilo Forest Reserve (4.92 S latitude, 38.66 E longitude).

Figure 2. The Worldview-2 image. Left: the entire image. Right: a small portion, approximately 900 m x 600 m on the ground, covering open land with scattered trees and a part of the Nilo Forest Reserve, Tanzania.

Time series analysis

A hidden Markov model is used to model each location on the ground as being in one of four states:

1.   forest

2.   sparse forest

3.   grass

4.   soil

The term 'hidden' refers to the fact that the true land cover class is not known. However, we have observations, in the form of sequences of Landsat image pixels for each 30 m x 30 m area on the ground (Figure 3). These observations are used by the time series analysis algorithm to predict the most probable sequence of states for each 30 m x 30 m area on the ground. From this, forest state changes, say, from "forest" to "sparse forest", can be found to have occurred between two observations. This approach does not propagate errors, since the whole sequence of observations of a pixel is classified simultaneously. The current approach treats each pixel in isolation.

The Landsat TM image data (band 1-5, and 7) are modelled using class dependent multivariate Gaussian probability density functions, and the parameters (mean vector and covariance matrix) are estimated from data corresponding to each of the classes. The training data is manually selected in two Landsat images (one from 6 October 1986 and one from 1 February 2010), guided by the very high resolution Worldview-2 image (Figure 2).
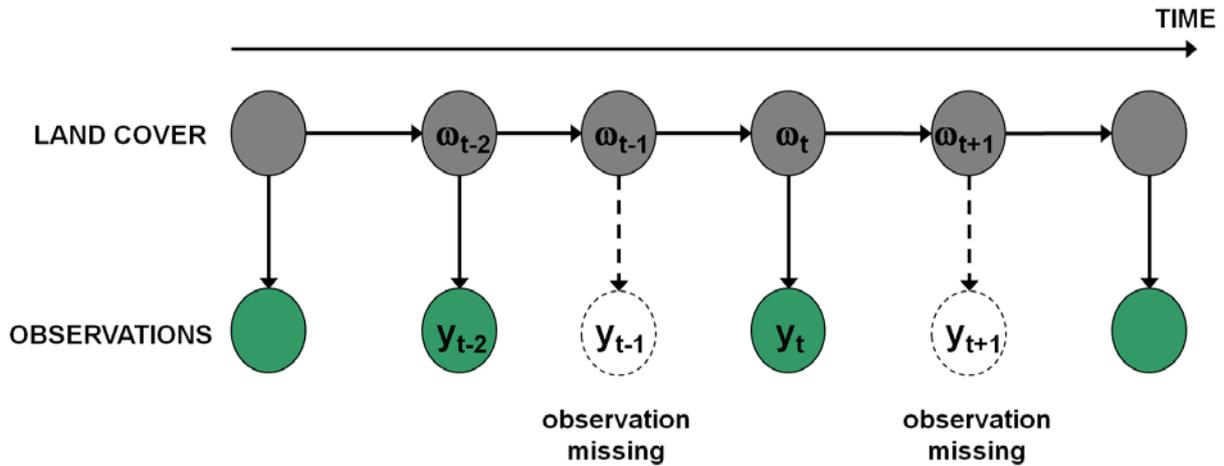
Figure 3. Principle of hidden Markov model. One area on the ground has a time series of hidden states, and each state may or may not have an associated observation. The hidden states are in grey, the observations are in green, and missing observations are indicated as dotted circles.
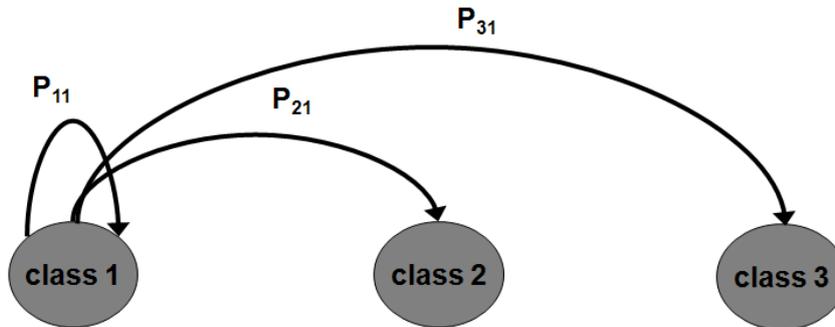

Figure 4. State transition probabilities for a hidden state that has class 1 in the present time instant.

The hidden Markov model is based on state or class transition probabilities (Figure 4). These need to be determined before we can classify the time series. These probabilities depend strongly on the application, and may be estimated from the data (14). The probabilities are designed to be dependent of the time interval between the two subsequent observations. At the moment, we have not estimated the transition probabilities from the data, but used time interval-dependent ad hoc values. For example,

$$P_{ij}(16\ days) = \begin{bmatrix} 0.9955 & 9 \cdot 10^{-5} & 2 \cdot 10^{-4} & 2 \cdot 10^{-4} \\ 9 \cdot 10^{-5} & 0.9955 & 2 \cdot 10^{-4} & 2 \cdot 10^{-4} \\ 0 & 0 & 0.977 & 0.0014 \\ 0 & 0 & 0.0014 & 0.977 \end{bmatrix} \ and\ P_{ij}(1\ year) = \begin{bmatrix} 0.9 & 0.09 & 0.005 & 0.05 \\ 0.09 & 0.9 & 0.005 & 0.005 \\ 0 & 0 & 0.7 & 0.3 \\ 0 & 0 & 0.3 & 0.7 \end{bmatrix}$$

where the four classes are given in the following order: forest, sparse forest, grass and soil.

Clouds and cloud shadows generally appear bright and dark, respectively, in the reflective bands. The cloud/shadow classification is performed using a support vector machine (SVM), with the C-parameter equal to one, and the smoothing parameter estimated using Silverman's mean integrated squared error method (15). Since cloud and cloud shadows are visually easily distinguished from vegetation, soil, etc., we assume that this classification task may be done with a very high accuracy. Pixels classified as clouds or cloud shadows are labelled as missing.

To reduce the impact of atmospheric variations between the images in the time series, we use the following method (16). The two training images are used as a baseline for the class-dependent distributions for the multispectral pixel values. For each of the remaining images and for each

class, the mean vector and covariance matrix of the class-dependent data distribution are adjusted such that the class mixture distribution possesses a good fit to the remaining images.

The processing chain may be summarized as follows: First the Landsat TM images (band 1-5, and 7) are converted to top-of-the-atmosphere (TOA) reflectance and the bands are stacked into one file. Then the SVM based cloud screening procedure is applied to the Landsat images. This procedure creates a mask corresponding to the pixels containing clouds or cloud shadows. The parameters corresponding to the class-dependent distributions are then re-trained for each image applied in the analysis. Now, the most likely or most probable state or class sequence $\Omega=\{\omega_1, \omega_2,\dots \omega_N\}$ is found for each pixel in stack of Landsat images by solving for Ω that maximizes the likelihood

$$p(\boldsymbol{x_1}, \boldsymbol{x_2}, \dots, \boldsymbol{x_N}|\Omega)p(\Omega) = \prod_{t=1}^{N} p(\omega_t|\omega_{t-1})P(\boldsymbol{x_t}|\omega_t)$$

using the efficient Viterbi algorithm (17). Here, $P(x_t|\omega_t)$ is the probability of observing the multispectral pixel value $\boldsymbol{x_t}$, given that the true state is ω_t. Each $P(x_t|\omega_t)$ distribution is estimated from the training data, assuming a multivariate Gaussian distribution. In practice, we have selected areas in the two images where no apparent change in land cover has taken place, and used the Worldview-2 image to locate specific areas of each class. The transition probabilities $p(\omega_t|\omega_{t-1})$ are taken from the transition probability matrix of the specific time delay between t-1 and t.
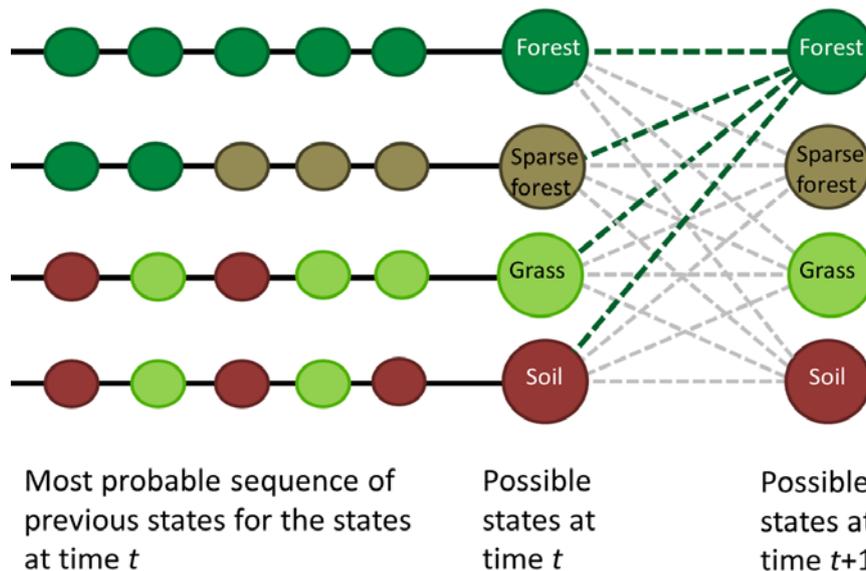

Figure 5. The most probable sequence at time t+1 for each state (e.g., forest) can be found by only considering the possible states at time t, since the most probable sequence of states for each state at time t is already known.

The brute force method of finding the most probable sequence of states, given the observations, is to examine all K^N (with K = number of classes = 4) possible sequences. However, the Viterbi algorithm is much faster than this, and works as follows. Let us assume that at time instant t, and for each of the K possible states, or classes, at a that specific time t, the most probable sequence of states leading to that specific state has been found. Then, the most probable sequence of states at time t+1 for state k at time t+1 can be found by comparing K expressions and selecting the maximum (Figure 5).

$$\Pr[bestsequence(t+1, k)] = \max_{c=1,..,K} \{\Pr[bestsequence(t, c)] P(\omega_{t+1} = k | \omega_t = c) P(\boldsymbol{x}_{t+1} | \omega_{t+1} = k)\}$$

This determines the most probable sequence at time t+1 for arriving at this state at time t+1. At each time instant, K^2 computations are done, giving a total of NK^2 instead of K^N computations. The state at t=0 is unknown, since the first observation is at t=1, so

$$p(\omega_1 | \omega_0) = p(\omega_1)$$

for all states k=1, …, K. $p(\omega_1)$ is then the prior probability of each state, and we have used equal prior probabilities for all states, i.e.

$$p(\omega_1) = 1/K$$

RESULTS

The method is applied on the time series of 14 Landsat images, and a small portion is inspected and compared with the Worldview-2 image. The method is able to pick up changes in an area where, at least by visual inspection of the Landsat images, there seems to have been a change in land cover from forest to non-forest. However, there are areas in the Worldview-2 image (4 March 2010) that appear as non-forest vegetation that are labeled as forest at the end of the time series (10 February 2010). E.g., see the 11 pixles 'forest' area in the land cover classification result of 10 February 2010 (Figure 6), which appears as an area with low green vegetation and a single, central tree canopy in the Worldview-2 image.
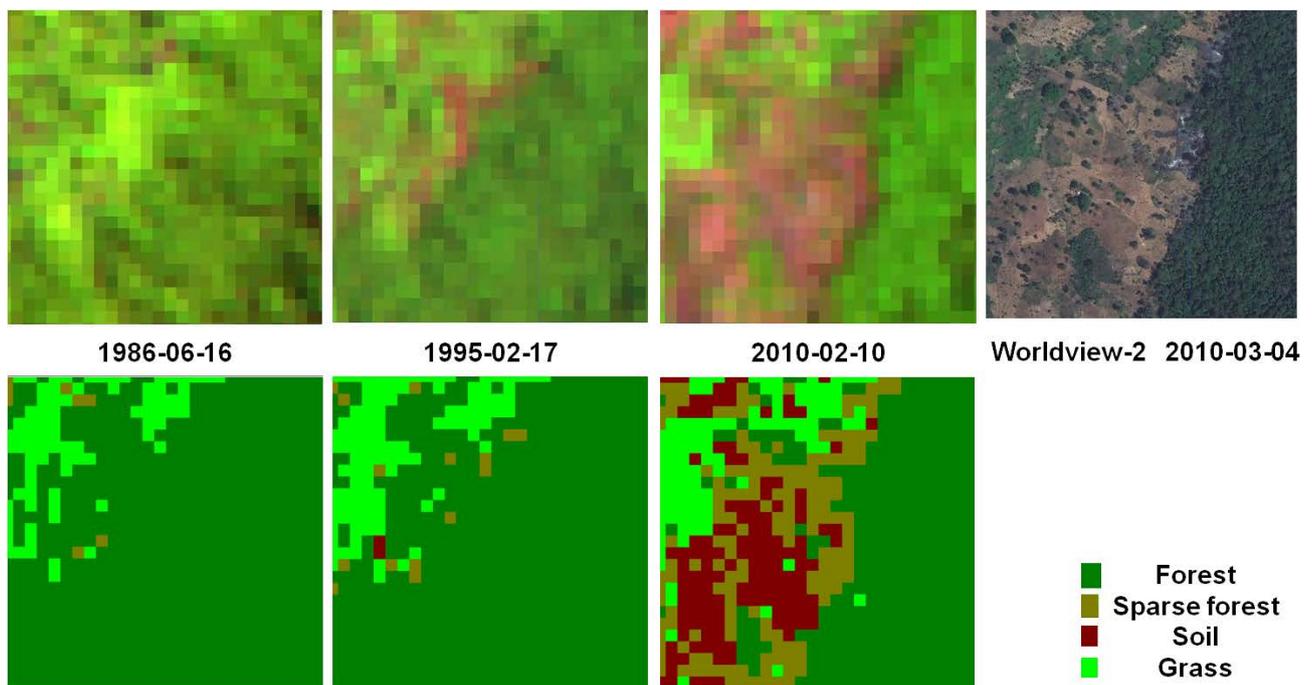

Figure 6. Result of land cover classification. Top row, from left: Landsat-5 images from 16 June 1986, 17 February 1995, and 10 February 2010; Worldview-2 image from 4 March 2010. Bottom row, from left: land cover classification results from 16 June 1986, 17 February 1995, and 10 February 2010.

The land cover classification maps are based on the most probable sequence of states for each individual pixel (Figure 7). From these sequences, change maps are also produced (Figure 7), showing some small changes from forest to non-forest between 1985 and 1995, and a large area of change between 1985 and 2009. In the event of missing observations, typically due to cloud

cover, the previous states are kept (Figure 8). The final change map shows a non-forest area (grey and red pixels) that is clearly smaller than the non-forest area in the Worldview-2 image.
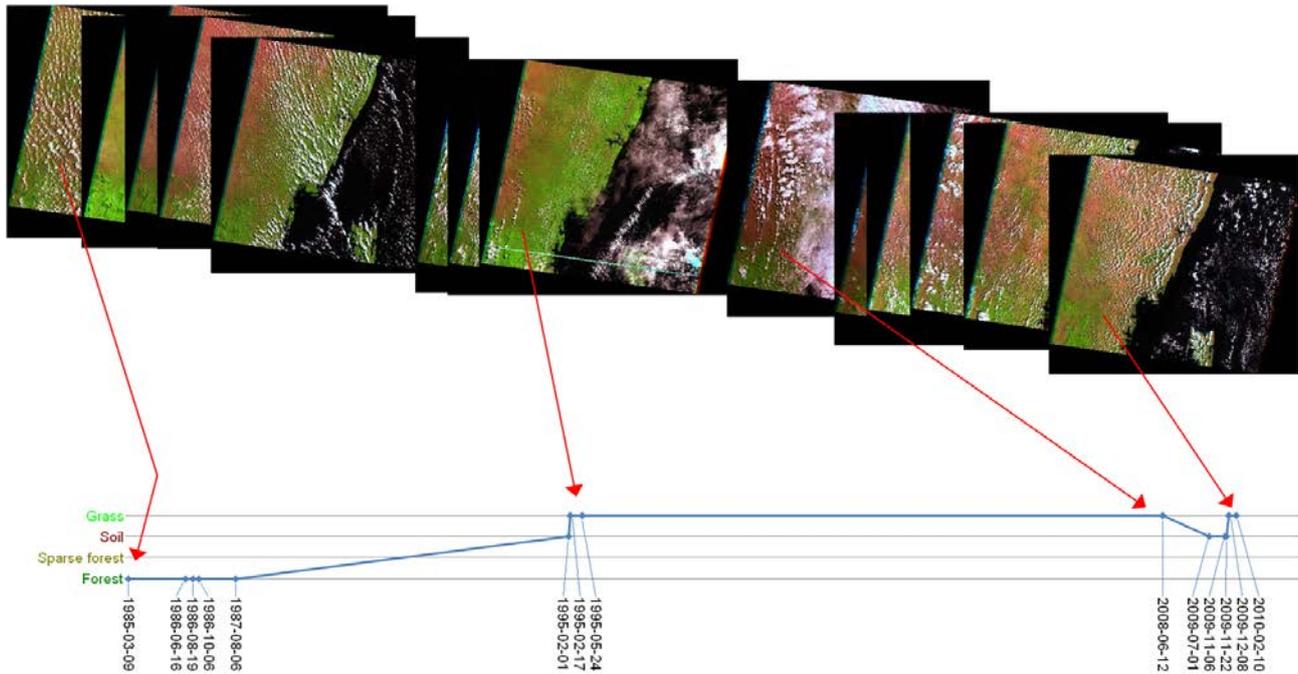

Figure 7. The most probable sequence of states for a single pixel.
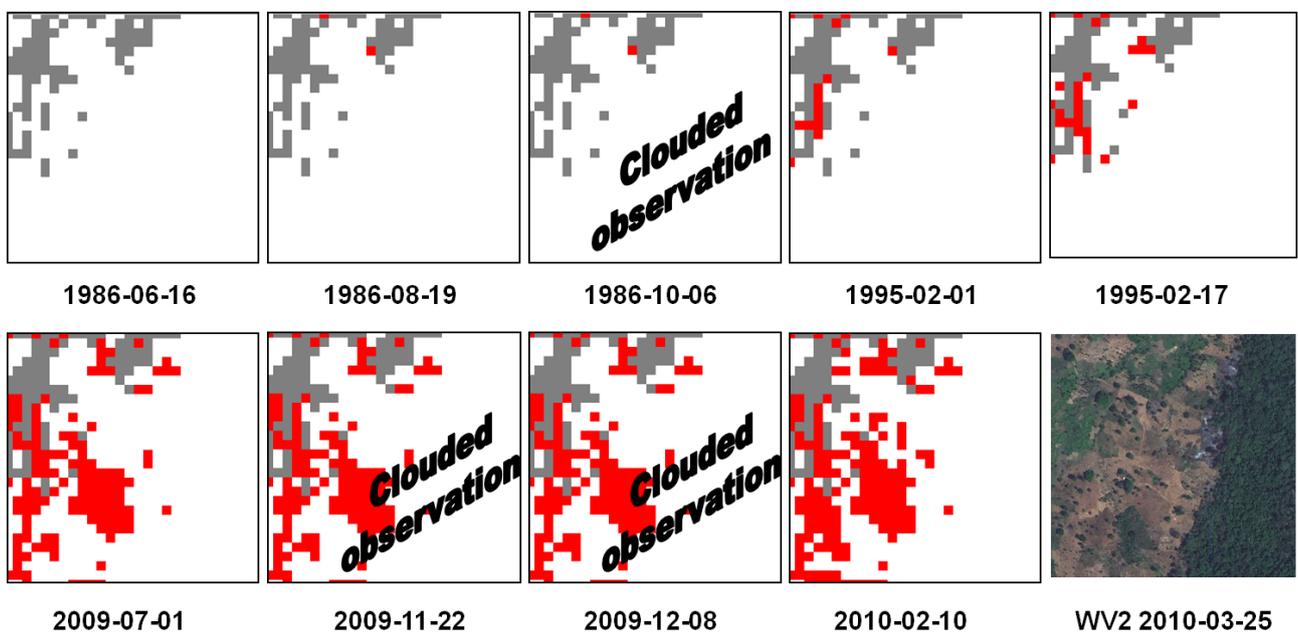

Figure 8. Change maps, relative to 9 March 1985. White: forest, grey: non-forest, red: changed from forest to non-forest. For three of the dates, cloud cover resulted in missing observations. Bottom right: Worldview-2 image of the same area inserted for reference.

DISCUSSION AND CONCLUSIONS

The purpose of the experiments was to get some indication of the suitability of a time series approach for forest change mapping, and to identify possible improvements. Many of these possible improvements will be addressed in the present project.

The experiments demonstrate that the method is able to detect changes from forest to non-forest, but that the total forest area seems to be overestimated. This may be due to limited training and some model assumptions. First of all, a more rigorous training of the method needs to be done. We will get access to a land cover map, in the form of ESRI shape file polygons, that was created by visual inspection of Landsat images from around 1995. We also expect to get access to a land cover map, based on field inspection and Landsat images from 2010, that will be completed near the end of 2011. This will make automatic training of the method possible, based on Landsat images from 1995 and 2010 and the land cover polygons.

Another potential improvement is better atmospheric correction. The current approach could be replaced by a more advanced method, e.g., by using the LEDAPS preprocessing tool to obtain ground surface reflectance (18). Further, the current cloud and cloud shadow detection method needs improvement.

Clearly, there are details in the Worldview-2 image, like individual trees, that cannot be seen in the Landsat image. One cannot expect the method to capture details that are not visible in the Landsat images. On the other hand, very high resolution images from Quickbird and Worldview-2 reveal that many Landsat pixels are mixed pixels of tree canopies, soil, low vegetation, etc. Very high resolution images are essential to identify mixed and pure Landsat pixels for training and testing of the methods

Due to varying cloud cover across a scene, and missing pixels (SLC-off) in Landsat 7 due to sensor failure, the different pixels may have different time series of observations. The hidden Markov model automatically compensates for this. However, the accuracy will increase with more observations, so it is important to have access to a dense time series of past observations, and guaranteed access to future acquisitions at regular and relatively short time intervals. The upcoming Landsat-8 and Sentinel-2 optical satellites will be important in this respect.

We observe that many of the Landsat images in the time series used in this study are contaminated with clouds. To overcome this, the Landsat time series could be supplemented with synthetic aperture radar (SAR) images, since the radar signals can penetrate all but the thickest clouds. However, SAR images are more difficult to interpret than optical images. Also, SAR backscatter is affected by humidity on the ground cover, and, for short wavelengths like C-band and X-band, whether deciduous trees have leaves or not. Consequently, forest cover mapping is not expected to perform well on individual images, calling for time series analysis of repeated SAR acquisitions. The time series analysis is expected to produce more accurate change detection and land cover classification than the processing of individual images. Further, since SAR and optical sensors measure different qualities of the land cover, they provide complementary information.

Thus, it can be expected that combining optical and SAR images will produce more accurate results than using only optical or only SAR. Several studies have confirmed this (e.g., see (19,20). The hidden Markov model approach is well suited for a mixture of optical and SAR observations (Figure 9).

In conclusion, we have demonstrated that time series analysis of each pixel based on a hidden Markov model is a promising method for forest change mapping. The Viterbi algorithm is used to find the most likely sequence of land cover classes for each pixel. The hidden Markov model handles missing observations due to cloud cover. The proposed method needs to be improved, both by more thorough training and by estimating the state transition probabilities from the data. Also, better pre-processing methods for atmospheric correction and cloud and cloud shadow detection are needed. Further, to reduce the impact of cloud cover, the method could be extended

to accept a mixture of optical and SAR images in the time series. We plan to do all this within the project.
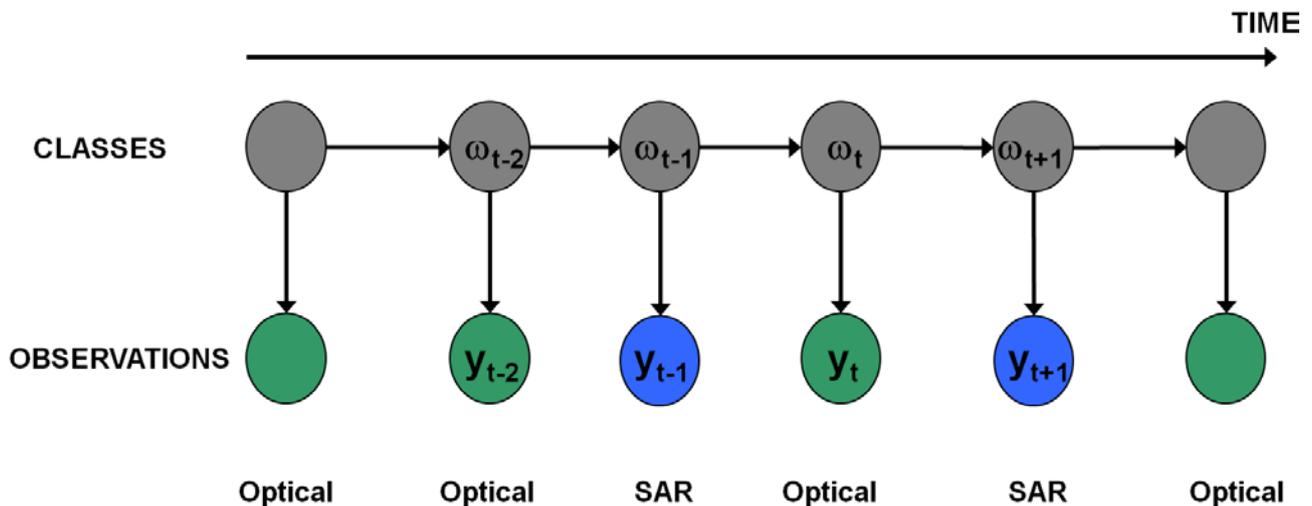

Figure 9. Extension of the hidden Markov model to multi sensor observations.

ACKNOWLEDGEMENTS

REFERENCES

1. Liang, S., Fang, H., Chen, M., 2001. Atmospheric correction of Landsat ETM+ land surface imagery – Part I: Methods. *IEEE Transactions on Geoscience and. Remote Sensing* 39(11), pp. 2490-2498.

2. Kaufman, Y. J., Wald, A., Remer, L. A, Gao, B., Li, R., Flynn, L., 1997. The MODIS 2.1 μm channel – correlation with visible reflectance for use in remote sensing of aerosol. *IEEE Transactions on Geoscience and Remote Sensing* 35, pp. 1286-1298.

3. Huang, C., Goward, S. N., Masek, J. G., Gao, F., Vermote, E. F., Thomas, N., Schleeweis, K., Kennedy, R. E., Zhu, Z., Eidenshink, J. C., Townshend, J. R. G., 2009. Development of times series stacks of Landsat images form reconstructing forest disturbance history. *International Journal on Digital Earth* 2(3), pp. 195-218.

4. Roy, D. P., Ju, J., Lewis, P., Schaaf, C., Gao, F., Hansen, M., Lindquist, E., 2008. Multi-temporal MODIS-Landsat data fusion for relative radiometric normalization, gap filling, and prediction of Landsat data. *Remote Sensing of Environment* 112, pp. 3112-3130.

5. Irish, R. I., Baker, J. L., Goward S. N., Arvidson, T., 2006. Characterization of the Landsat-7 ETM+ automated cloud-cover assessment (ACCA) algorithm. *Photogrammetric Engineering & Remote Sensing* 72, pp. 1179-1188.

6. Hégarat-Mascle, S. L., André, C. (2009). Use of Markov Random Fields for automatic cloud/shadow detection on high resolution optical images. *ISPRS Journal on Phogrammetry and Remote Sensing* 64, pp. 351-366.

7. Huang C., Goward, S. N., Masek, J. G., Thomas, N., Zhu, Z., Vogelmann, J. E., 2010. An automated approach for reconstructing recent forest disturbance history using dense Landsat time series stacks. *Remote Sensing of Environment* 114, pp. 183-198.

8. Aurdal, L., Huseby, R. B., Vikhamar, D., Eikvil, L., Solberg, A. H. S., Solberg, R., 2005. Classification of multitemporal satellite images using phenological models. In: Third International Workshop on the Analysis of Multitemporal Remote Sensing Images, pp. 220-224.

9. Leite, P. B. C., Feitosa, R. Q., Formaggio, A. R., da Costa, G. A. O. P., Pakzad, K., Sanches, I. D.A., 2011. Hidden Markov models for crop recognition in remote sensing image sequences. *Pattern Recognition Letters* 32 (1), pp. 19-26.

10. Salberg, A.-B., 2011. Land cover classification of cloud-contaminated multitemporal high-resolution images. *IEEE Transaction on Geoscience and Remote Sensing* 49 (1), pp. 377-387.

11. Theodoridis S., Koutroumbas K., 1999. *Pattern Recognition.* Academic Press, San Diego, California.

12. van der Heijden, F., Duin, R. P. W., de Ridder, D., and Tax, D. M. J., 2004. Classification, Parameter Estimation and State Estimation. Chichester, England: Wiley.

13. Bahl, L., Cocke, J., Jelinek, F., Raviv, J., 1974. Optimal decoding of linear codes for minimizing symbol error rate. *IEEE Transactions on Information Theory* 20(2), pp. 284–287.

14. Rabiner, L. R., 1989. A tutorial on hidden Markov models and selected applications in speech recognition. *Proceedings of the IEEE* 77 (2), pp. 257-286.

15. Silverman, B. W., 1986. Density Estimation for Statistics and Data Analysis. Chapman and Hall, London.

16. Salberg, A.-B., 2011. Retraining maximum likelihood classifiers using a low-rank model. *IEEE International Geoscience and Remote Sensing Symposium*, Vancouver, Canada, 24-29 July 2011.

17. Salberg, A.-B., Trier, Ø. D., 2011. Temporal analysis of forest cover using hidden Markov models. *IEEE International Geoscience and Remote Sensing Symposium*, Vancouver, Canada, 24-29 July 2011.

18. Masek, J., G., Vermote, E. F., Saleous, N. E., Wolfe, R., Hall, F. G., Huemmrich, K. F., Gao, F., Kutler, J., Lim, T.-K., 2006. A Landsat surface reflectance dataset for North America, 1990-2000. *IEEE Geoscience and Remote Sensing Letters* 3 (1), pp. 68-72.

19. Solberg, A. H. S., 1999. Contextual data fusion applied to forest map revision. *IEEE Transaction on Geoscience and Remote Sensing* 37, pp. 1234-1243.

20. Storvik, B., Storvik, G., Fjørtoft, R., 2009. On the Combination of Multisensor Data Using Meta-Gaussian Distributions. *IEEE Transactions on Geoscience and Remote Sensing* 47 (7), pp. 2372-2379.